Detection of Thin Cracks on Noisy Pavement Images

LAN LI, PAUL CHAN, AND ROBERT L. LYTTON

One of the challenging problems in the area of automatic interpretation of the pavement condition videos or images is detecting the presence of low- to medium-severity cracking when the mean crack width is less than ¼ in. This problem is further complicated by the texture of the background pavement. The variations in light intensity between aggregates and bituminous material are similar to that of the actual cracking (noisy images). The traditional approach to solving this problem includes three techniques. The first is to increase the resolution of the video camera by using a higher resolution camera or alternatively by recording the pavement image on super VHS tapes. The second technique that is often used in noisy images is applying a low-pass filter to remove the pixels with rapid intensity variations between them (inevitably reducing the sharpness of edges). The third technique involves the use of a localized edge detector by which local edge points can be detected in small subareas. The shortcoming of the third technique is that it includes isolated noisy spots as edge points. Development of an innovative technique on edge detection is based on the Sobel operation coupled with Kittler's automatic thresholding and a sequence of postprocessing operations. Image examples of thin cracks on asphalt concrete and PCC surfaces are used to demonstrate the capability of this image analysis technique.

Pavement distress data are critical to all pavement management activities. Promptly collected and analyzed pavement distress data can assist a pavement system engineer in making plans and decisions. In the past, pavement distress surveys were conducted by a team of two pavement raters. This team would drive or walk along the shoulder of a road to visually evaluate the surface condition of the pavement (*1–3*). With the advancement of video technology, the current process of pavement distress surveying uses photologging of pavement surfaces on 35-mm high-speed film, video tape, or video disc. This process allows pavement surface inspection to be done indoors, which saves time and money. It also reduces the safety hazard the survey crew faces in the field.

After improving surveying techniques, the next logical step is to develop image analysis and pattern recognition algorithms to process the digital images of pavement surfaces (*4,5*). This process will include identifying and quantifying major pavement distress types. The problem with identifying and quantifying cracks is noise in the image. As compared with any other real life images, pavement images are noisy. A crack in a pavement image is observed as a variation of grey level. In order to automatically locate cracks, gradient operators are frequently used to monitor the change in intensity between pixels and thus to enhance any crack and to detect edges. The two most common edge operators are the Roberts gradient (*6*) and Sobel operators (*7*). Roberts gradient, which is simply the sum of the cross-differences in a 2×2 region, is susceptible to noise. Sobel operators are 3×3 area operators in which the weights for the two neighbor pixels of the middle pixel is two. This set of multipliers has the effect of smoothing the image and results in less sensitivity to noise.

An important calculation required in processing pavement images is the automatic threshold calculation. But thresholding with a histogram requires a bimodal or multimodal distribution, which are unlikely in pavement images.

Texas Transportation Institute, College Station, Tex. 77843–3135.

THIN CRACK DETECTION AND MEASUREMENT METHOD

In Texas, longitudinal and transverse cracks with mean width less than 0.25 in. are considered to be of low severity level. The images that are collected by the Texas State Department of Highways and Public Transportation are of full-lane width (i.e., about 12 ft). A digitized video image has 512×480 picture elements (pixels). Each pixel corresponds to about 0.23 in. A grey level value is assigned to each pixel in the digitization process, with 255 representing the brightest light level and 0 the darkest. The profile of the grey level for an image of a thin crack usually exhibits a valley or a dip. For a thin crack, the change of grey level can be small and subtle. This problem is further complicated by the grainy look of the intact pavement in the background.

An innovative algorithm has been developed to identify a thin or a low-severity crack on pavement surfaces. Figure 1 shows the major building blocks of this algorithm; the following sections will give detailed discussions of each. As a grey level image input into this algorithm, the edges are extracted with the Sobel edge operators in the image statistics acquisition. The image statistics will include the estimates for the noise in the image; this information is used in the calculation of the threshold level. After the pavement image is segmented into a binary image, a sequence of postprocessing steps is carried out to quantify thin cracks. These procedures include the elimination of noisy spots, scanning of the crack segment, tracing of the boundary of the crack segment, and determination of the orientation of this segment. After the linking of crack segments, the length and width of the crack are then calculated.

EDGE DETECTOR

An edge detector is used to locate the change of the grey level in an image. Sobel edge detectors are chosen on the

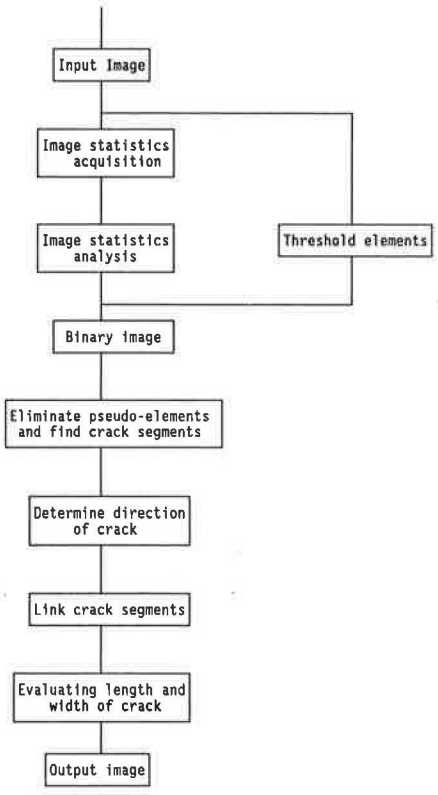

FIGURE 1 Block diagram of thin crack detection and quantifying algorithm.

basis of the fact that they are an area operator that can suppress random and isolated noisy spots. Figure 2 shows the horizontal and vertical masks (i.e., sets of weighting factors). The horizontal mask is used to extract the horizontal edge element, the vertical mask to extract the vertical edge element. The magnitude of the horizontal gradient of a pixel is expressed in terms of the weights in the horizontal mask.

$$|e_{xi,j}| = |-f_{i-1,j-1} - 2f_{i,j-1} - f_{i+1,j-1} + f_{i-1,j+1} + 2f_{i,j+1} + f_{i+1,j+1}| \quad (1)$$

Similarly, the magnitude of the vertical gradient can be computed as

$$|e_{yi,j}| = |-f_{i-1,j-1} - 2f_{i-1,j} - f_{i-1,j+1} + f_{i+1,j-1} + 2f_{i+1,j} + f_{i+1,j+1}| \quad (2)$$

-1	-2	-1
0	0	0
1	2	1

Horizontal Mask

-1	0	1
-2	0	2
-1	0	1

Vertical Mask

FIGURE 2 Horizontal and vertical Sobel masks.

The gradient for a pixel is the maximum value of the horizontal gradient and vertical gradient

$$|e_{i,j}| = \max(|e_{xi,j}|, |e_{yi,j}|) \quad (3)$$

THRESHOLD CALCULATION

After a gradient image is obtained from the Sobel edge operator, an automatic threshold level determination technique suggested by Kittler (*8–10*) is adopted. For an ideal image of an object with uniform grey level f_0, and the grey level for the background f_b, the ideal threshold level should be $(f_0 + f_b)/2$. The threshold selection is based on the following formula.

$$T = \frac{\sum_i \sum_j f_{ij}\, e_{ij}}{\sum_i \sum_j e_{ij}} \quad (4)$$

In Equation 4, the grey level of each pixel (f_{ij}) is multiplied by its gradient (e_{ij}); in other words, it is weighted with the corresponding gradient. This equation calculates the ideal threshold level in an ideal image. (Most images are nonideal, especially pavement surface images in which the aggregates for the pavement surface demonstrate naturally noisy images.) Kittler has suggested a technique to estimate a statistical parameter for the noise and exclude the effect of noise in the threshold calculation. This technique estimates the standard deviation of the gradients measured assuming the noise has a Gaussian distribution. Only the pixels with gradients greater than six times the estimated standard deviation are included in the calculation of the threshold value. Kittler (*9*) has demonstrated experimentally for the case of a small object that $6\hat{\sigma}$ is the optimal value used in the threshold calculation for background noise rejection. This process ensures that only true edge pixels are involved in the determination of the threshold. Figure 3 shows the effect of this noise rejection scheme. Figure 3a shows a normal picture of a longitudinal crack. The image shown in Figure 3b is the result of the Sobel

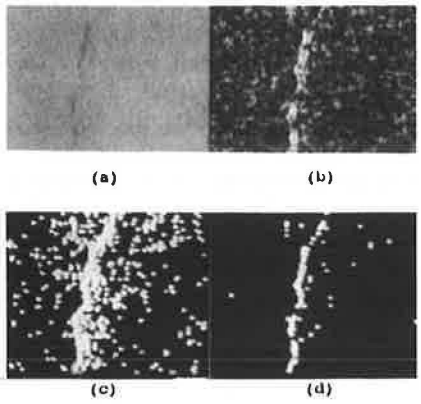

FIGURE 3 Effects of the noise rejection scheme: (a) original longitudinal crack, (b) result of the Sobel operator with edge enhanced, (c) result of processing with Kittler's original threshold method, and (d) result of processing with modified method.

operators with edges enhanced. The results from processing with Kittler's original threshold method and modified method are shown in Figures 3c and 3d, respectively.

POSTPROCESSING

The complexity of pavement image analysis can be grouped into three categories. The first is the variability of the material used in the building of the pavement, such as the color of aggregates, the shape and size of aggregate, and the amount of asphalt cement. The second is the different forms and shapes of the distress types that are supposed to be quantified. The last group that is added to the challenging nature of pavement image analysis is the presence of various nondistress objects such as tire marks, paint stripes, shadows, and others. The binary image obtained from the Sobel edge detector and the Kittler automatic thresholding inevitably has some random noisy pixel points and short noncrack elements (a group of noisy pixel points) as well as the actual cracking itself. The postprocessing techniques remove the noisy pixel points and isolate short elements to provide more accurate measurement of the width and length of the thin crack. The postprocessing can be divided into four parts.

1. Removal of the Noisy Pixels. The random noisy pixels that appeared as white dots in the binary image are contributed by the rough texture of the pavement surface. They can be differentiated from the real cracking on the basis of the perimeter of the pixel group as indicated in the next paragraph.
2. Location and Identification of Crack Segments. A thin crack usually has a defined width and a continuous array of edge pixels and all pixels may have similar grey levels. After thresholding, the thin crack may appear as broken pieces of crack segments. A boundary searching algorithm (*11*) is applied to find the boundary (perimeter) of the object. This scheme not only locates the crack segments but also deletes the isolated noisy pixels according to the threshold set for the perimeter. A threshold value of 20 is used for the perimeter, where the selection is based on the trade-off between noisy spots and short segments. If the threshold is set too high, real short crack segments will be discarded. On the other hand, if the threshold is set too low, noisy spots will appear. Figure 4c shows the image with crack segments, with noisy pixels resulting from binary thresholding. The resulting image (Figure 4d) indicates the removal of noisy pixels on the basis of magnitude of the perimeter. Because the display contrast setting for the binary image in Figure 4c is high, the isolated noisy spots that are in close proximity to the crack segments are easily misconceived to be part of the crack segments. Once these spots are removed on the basis of the determined threshold for the boundary length, the details of the crack segment in Figure 4d appear different from those of its predecessor. These differences can be observed as thinner crack widths or shorter crack segments.
3. Connection of Crack Segments to Form the Crack. As the binary thin crack image is scanned and the boundary of a crack segment is traced out, the characteristic points of the crack segment are also recorded. These points include the location of the center of gravity, which can be approximated by the average of all the coordinate pairs that form the boundary of the crack segments. Furthermore, the smallest and largest coordinate pairs in the horizontal as well as in the vertical direction can be used to connect to other crack segments. The orientation of the crack segment is usually in agreement with that of the whole crack; this information will lead to determining how and where the crack segments are connected. Furthermore, a threshold distance is determined experimentally to connect close short segments while rejecting short noisy spots in parallel with real cracking that are usually farther away. For example, a transverse crack segment will connect from its largest horizontal point to the right and smallest horizontal point to the left. Finally, the thin crack is reconstructed from a set of crack segments and connecting straight lines. Figure 4f shows the result of the technique. The current connection method is only suitable for longitudinal and transverse cracking. Further research efforts will be required to quantify the extent of alligator cracking where linear cracks cross one another in an irregular pattern.

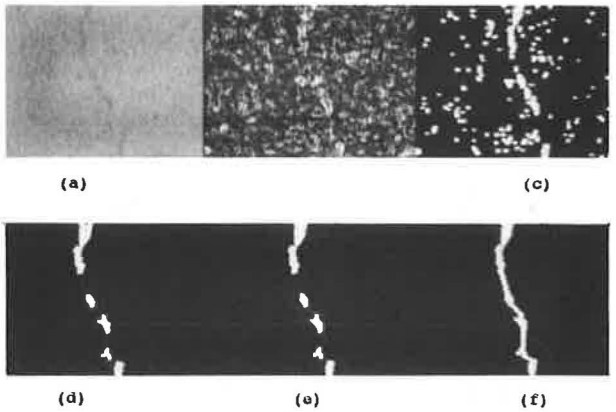

FIGURE 4 Illustration of thin crack detection: (a) original crack image, (b) result of the Sobel operator with edge enhanced, (c) image with crack segments, (d) image after removing noisy pixels and elements, (e) boundary image of crack segments traced out, and (f) final result of detecting crack.

4. Estimation of Lengths and Mean Widths of Thin Cracks. The crack lengths and mean widths are usually recorded on pavement surface evaluation data sheets. The ability to detect thin cracks is not only based on the image analysis algorithm but also on the resolution and field of view of the video camera. Detection of thin cracks or even hairline cracks (i.e., in a higher-resolution camera or a smaller field of view) provides vital information for early warning of road surface condition. The crack lengths and mean widths can be estimated from two methods.

1. The length is estimated by adding all the connecting straight lines and all the lengths of the crack segments. The mean crack width is calculated by dividing the crack area by the crack length. The crack area is estimated by summing the area of the crack segments and all the connecting straight lines, assuming a width of one pixel.
2. This method is similar to the preceding one with the exception that the length of the crack is approximated as the line joining the first crack to the last crack segment.

A set of mat boards with different sizes of graphic tape attached to each board was used to calibrate the image pro-

cessing and analysis system. Tape widths of ⅛, ¼, and ½ in. were attached to three individual boards and an image of each was obtained. In order to simulate the random orientation of pavement cracking, images with each tape line positioned at five different angles were obtained. The calculated width at each direction is compared with the known width and an average percent error is calculated. About 20 percent is found for the ½-in. uniform width, whereas the percent error for ¼ in. is as high as 100 percent. The main reason for this high error rate is that the highest resolution for this particular camera and image processing system is 0.23 in. In other words, when a coverage of 10- × 10-ft area is digitized into 512 × 480 elements (pixels), the theoretical size of the smallest object that can be detected is 0.23 × 0.23 in. With the presence of noise, camera distortion, and spatial quantization error, the total percent error will be unacceptable for object detection for an object of width one pixel. It is recommended that the desired smallest crack width should be at least two pixels for crack detection.

EXPERIMENTAL RESULTS AND ANALYSIS

In order to test this algorithm, three images of asphalt surface and four images of PCC road surface were chosen. The three evaluation criteria are as follows: (a) how well this algorithm can detect the presence of a thin crack, (b) how accurate is the estimation of the length and width of the crack, and (c) how it performs for different pavement types. The pavement surface images that are recorded by the automatic road analyzer (ARAN) covered a trapezoidal area of 8 ft of upper side, 14 ft of lower side, and a latitude of 10 ft. This area is mapped onto a digital image with 512 horizontal pixels and 480 vertical pixels. Each pixel width corresponds to about 0.23 in. after the geometric compensation is considered. The extracted test images are 128 × 128 pixels representing about 6.25 ft². Figures 5a through 5g show the originals and the results processed with this algorithm. Table 1 presents the computed lengths and mean widths for the linear crackings of asphalt pavement surfaces. Table 2 presents the mean width of a transverse crack on concrete pavement as well as the extents of three spalled cracks. The width and length of the spalled area are recorded to determine the severity of each crack.

Between the two methods that estimated the length of the thin crack, the single straight line method can compute the length in shorter time but is less accurate, whereas the mul-

TABLE 1 COMPUTERIZED EVALUATION OF THREE ASPHALT CRACKING IMAGES

Distress Type	Length (inch)	Mean Width (inch)	Severity Level
Longitudinal 1 Fig. 5(a)	17.66	0.36	Medium
Longitudinal 2 Fig. 5(b)	23.55	0.40	Medium
Transverse Fig. 5(c)	20.61	0.24	Low

Note:
Low Severity: Mean Crack Width < 1/4" .
Medium Severity: Mean Crack Width > 1/4" .

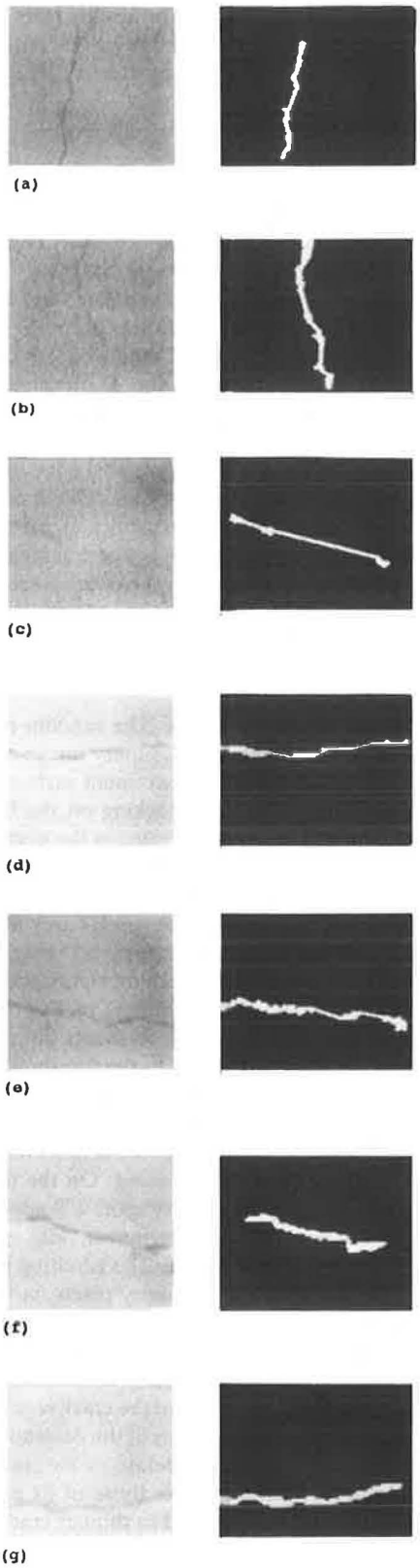

FIGURE 5 Examples in asphalt: (a), (b) longitudinal cracks, and (c) transverse crack. Examples in concrete: (d) transverse crack, (e)–(g) spalled cracks.

TABLE 2 COMPUTERIZED EVALUATION OF FOUR PCC CRACKING IMAGES

Distress Type	Mean Crack Width (inch)	Crack Length (inch)	Spall Width (inch)	Spall Length (inch)	Severity Level
Transverse Fig. 5(d)	0.46	23.37			Medium
Spalled crack1 Fig. 5(e)			1.10	0.66	Low
Spalled crack2 Fig. 5(f)			1.02	1.13	Low
Spalled crack3 Fig. 5(g)			1.02	1.24	Low

Note:
Transverse Crack
Low Severity: Mean Width < 1/8".
Medium Severity:1/8" < Mean Width <1".
Spalled Crack
Low Severity: Spalled width 1"--3".
Medium Severity:Spalled width >3".

tiply connected straight line requires longer computation time but yields more accurate length measurement. This trade-off can be studied further in detail when a length of roadway is processed.

Because of the complexity and variability of pavement surface images, the thin crack obtained from this algorithm may not resemble the original image perfectly. This effect will contribute to the error in the length estimation. On the other hand, the mean width calculation is based on the crack area as well as the estimated length measured from the image. For example, if an underestimated area is divided into an underestimated length, the result will actually yield a crack width with lower percent error. In order to rate the pavement surface condition, the knowledge of the severity of cracking, which is based on the mean crack width, is critical and the algorithm provides this value.

SUMMARY AND CONCLUSION

The Sobel edge detector and an automatic thresholding technique based on Kittler et al. (*9*), adding a sequence of postprocessing to identify and quantify low-severity-level cracking, have been described. From the examples, this technique has successfully detected and extracted the information for these thin cracks. The advantage of using an automatic threshold is that it does not rely on the needed bimodal distribution for threshold selection as in histogram thresholding. This technique has been found able to detect and quantify thin cracking despite the noisy background image. The resolution can be further improved using a higher resolution camera (1,024 × 1,024) and smaller coverage of the camera (6 × 6 ft), eventually allowing the detection of hairline cracks. This technique can quantify the length and width of the thin crack in an accurate manner, hence providing a tool for automatic pavement distress evaluation.

ACKNOWLEDGMENT

The authors would like to acknowledge the support of the Texas State Department of Highways and Public Transportation. Tom Scullion provided many helpful suggestions and detailed comments.

REFERENCES

1. R. E. Smith, M. I. Darter, and S. M. Herrin. *Highway Pavement Distress Identification Manual.* Report DOT-FH-11-9175/NCHRP 1-19. FHWA, U.S. Department of Transportation, 1979.
2. *Guidelines and Procedures for Maintenance of Airport Pavements.* Advisory Circular, AC 150/5380-6, FAA, U.S. Department of Transportation, 1982.
3. *1989 Pavement Evaluation System Rater's Manual.* Texas State Department of Highways and Public Transportation, Austin, 1989.
4. T. Fukuhara, K. Terada, M. Nagao, A. Kasahara, and S. Ichihashi. Automatic Pavement Distress Survey System. *Proc., 1st International Conference on Application of Advanced Technologies in Transportation Engineering*, ASCE, San Diego, Feb. 1989, pp. 33–38.
5. G. Caroff, P. Joubert, F. Prudhommee, and G. Soussain. Classification of Pavement Distresses by Image Processing (MACADAM SYSTEM). *Proc., 1st International Conference on Application of Advanced Technologies in Transportation Engineering*, ASCE, San Diego, Feb. 1989, pp. 46–51.
6. L. G. Roberts. Machine Perception of Three Dimensional Solids. *Optical and Electro-Optical Information Processing*, J. T. Tippet, ed., Massachusetts Institute of Technology Press, Cambridge, 1965.
7. R. C. Gonzalez and P. Wintz. *Digital Image Processing*, 2nd ed. Addison-Wesley, New York, 1987.
8. J. Kittler, J. Illingworth, and J. Foglein. Threshold Selection Based on a Simple Image Statistic. *Computer Vision, Graphics, and Image Processing*, Vol. 30, 1985, pp. 125–147.
9. J. Kittler, J. Illingworth, J. Foglein, and K. Paler. An Automatic Thresholding Algorithm and Its Performance. *Proc., 7th International Conference on Pattern Recognition*, 1985, pp. 287–289.
10. K. B. Chan, S. Soetandio, and R. L. Lytton. Distress Identification by an Automatic Thresholding Technique. *Proc., 1st International Conference on Application of Advanced Technologies in Transportation Engineering*, ASCE, San Diego, Feb. 1989, pp. 468–473.
11. P. Grattoni and R. Bonamini. Contour Detection of the Left Ventricular Cavity from Angiographic Images. *IEEE Transactions on Medical Imaging*, Vol. MI-4, No. 2, June 1985.

Publication of this paper sponsored by Committee on Pavement Monitoring, Evaluation, and Data Storage.